Research Article

Xiaotao Wang*, Zhuofan Chen, Yiwan Huang, Xiaotie Ye, Jiacheng Wang, Yuye Yang, Xuefeng Li, and Zuifang Liu*

Liquid crystallinity and thermal properties of polyhedral oligomeric silsesquioxane/side-chain azobenzene hybrid copolymer

https://doi.org/10.1515/ntrev-2020-0068
received June 27, 2020; accepted July 22, 2020

Abstract: Acrylic acid-modified polyhedral oligomeric silsesquioxane (AC-POSS) was synthesized by the reaction between the amine groups in polyhedral oligomeric silsesquioxane (POSS) and acrylic acid, which could dissolve in water and can be easily purified. Free-radical copolymerization was applied to synthesize azobenzene liquid crystalline polymer silsesquioxane (LCP-POSS) with different proportions of AC-POSS and liquid crystalline monomers. The *trans*-isomers of azobenzene moieties in LCP-POSS were gradually transformed to *cis*-isomers with increasing ultraviolet irradiation time. The photoisomerization reaction of liquid crystalline polymer (LCP) and LCP-POSS showed the first-order dynamic reaction. Compared with the LCP, the photoisomerization rate constant of LCP-POSS was decreased due to the space steric hindrance of the POSS as a rigid segment. The phase transition temperature of liquid crystalline in LCP-POSS increased with increasing POSS content, and the liquid crystalline texture in LCP-POSS became smaller under the polarized light. With further increasing the POSS content (>50 wt%) in LCP-POSS, the ordered structure of the liquid crystalline phase was gradually affected, resulting in one-way liquid crystal (LC) phase behavior. The synthesized LCP-POSS has LC properties, light-responsive properties, and thermal stability. When the POSS is introduced into the LC material, the phase state of the LC material will become more abundant and the LC phase will become more stable. The significance of this study is to develop and extend its applications as stimuli-responsive materials and devices.

Keywords: polyhedral oligomeric silsesquioxanes, liquid crystalline behaviors, azobenzene, photo-isomerization, thermal stability

1 Introduction

Polyhedral oligomeric silsesquioxane (POSS) has attracted more attention due to the excellent thermal stability and processability in their hybrid organic–inorganic nanocomposites [1–8]. POSS with three-dimensional cage structure, consisting of three functional groups, is a kind of organic silicon compound synthesized through hydrolysis condensation [9–12]. Its chemical formula is $(RSiO_{1.5})_n$, where R is either hydrogen or alkyl, alkylene, aryl, or arylene group, and n takes values of 6, 8, 10, or 12. Typically, POSS nanoparticles are built by a stiff core with nanometer-sized (1–3 nm) and star-like supramolecular structures $(SiO_{1.5})_n$ of cage shape, where each atom of Si is surrounded by three oxygen atoms. The $(SiO_{1.5})_n$ core can be functionalized with different organic pendant groups [13–17]. Chemical copolymerization and physical blending are mainly utilized to prepare POSS-based polymer materials to

* **Corresponding author: Xiaotao Wang,** Hubei Provincial Key Laboratory of Green Materials for Light Industry, Collaborative Innovation Center of Green Light-weight Materials and Processing, and School of Materials and Chemical Engineering, Hubei University of Technology, Wuhan, Hubei, 430068, People's Republic of China, e-mail: xiaotaowang@hbut.edu.cn
* **Corresponding author: Zuifang Liu,** Hubei Provincial Key Laboratory of Green Materials for Light Industry, Collaborative Innovation Center of Green Light-weight Materials and Processing, and School of Materials and Chemical Engineering, Hubei University of Technology, Wuhan, Hubei, 430068, People's Republic of China, e-mail: zuifang@yahoo.co.uk
Zhuofan Chen, Yiwan Huang, Jiacheng Wang, Yuye Yang, Xuefeng Li: Hubei Provincial Key Laboratory of Green Materials for Light Industry, Collaborative Innovation Center of Green Light-weight Materials and Processing, and School of Materials and Chemical Engineering, Hubei University of Technology, Wuhan, Hubei, 430068, People's Republic of China
Xiaotie Ye: Lingyun Technology Group Co. Ltd, Wuhan, Hubei, 430040, People's Republic of China

improve their thermal stability due to the presence of POSS [18–22].

Liquid crystalline polymer (LCP) has attracted increasing attention due to its molecular orientation order, and POSS also has the ability of self-assembly with its regular structure. The incorporation of POSS may benefit the formation of the liquid crystal (LC) order. Kim et al. [23] prepared LCP-containing POSS by random copolymerization between vinyl-containing single functional group of POSS and one side chain type LC monomers. When the feed ratio of the POSS monomer is greater than 10%, the resulting LCP does not have LC properties. Compared with the LC homopolymer, the phase transition temperature of the LC copolymer decreased and the stability of the LC phase increased. Fan et al. [24] investigated that hybrid organic–inorganic jacketed polymers containing two POSS moieties in the side chains, denoted as P_nPOSS (n = 6 or 10, the number of methylene units between the terephthalate core and POSS moieties in the side chains), which were synthesized through conventional free radical polymerization. Compared with the triphenylene discotic LCs, crystalline POSS moieties have a stronger tendency of aggregation and can stabilize the LC phases formed by mesogen-jacketed LCPs. Laine et al. [25] reported the POSS with average of four LC motifs in each molecule, which has only nematic phase. An LC material with both nematic and smectic crystalline phases containing an average of five LC elements in the molecule was prepared by controlling the feed ratio [26]. The incorporation of POSS into LCP increased the liquid phase transition temperature and enriched the LC phase.

The azobenzene polymer has attracted wide attention due to its photoluminescence property. Under ultraviolet (UV) irradiation, *trans–cis* configuration conversion could occur, while the molecular configuration restores to *trans*-structure under visible light or heated effect [27]. The structure and performance characteristics of azobenzene were studied deeply [28–32]. Chen et al. [33] prepared the functional POSS-based fluorinated azobenzene polymers, which were expected to be applied on the surface with light-responsive properties with controlled wettability. Miniewicz et al. [34] reported a novel polymer of polymethyl methacrylate composite dispersed with azo-functionalized POSS nanoparticles with photoresponsive properties.

However, there are no studies on the POSS and azobenzene LC hybrid nanomaterial with different POSS contents through free radical polymerization to discuss the azobenzene LC phase behavior under the confinement of different POSS contents [35]. The LCP-POSS has LC properties, light-responsive properties, and thermal stability. In this study, POSS with different proportions was incorporated into azobenzene LCP through free-radical polymerization. When the POSS is introduced into the LC material, the phase state of the LC material will become more abundant and the LC phase will become more stable. Meanwhile, the influence of POSS on the light-responsive properties of azobenzene has been studied, and LCP photoisomerization rate constant was investigated. Azobenzene LCP has photoisomerization properties, which could be applied in nanodevice, optical switch, information storage, and liquid crystal display. The LC phase and the thermal stability might be enhanced by the incorporation of low content of POSS to some extent, which may promote and extend its applications as stimuli-responsive materials and devices.

2 Materials and methods

2.1 Materials

Aminopropylisobutyl polyhedral oligomeric silsesquioxane (AC-POSS) was obtained from Hybrid Plastics, Inc. Dimethylformamide (DMF) was purified by vacuum distillation before use. High-purity 2,2-azobisisobutyronitrile (AIBN) was recrystallized from 95% ethanol. Spectroscopic grade tetrahydrofuran (THF) and toluene were pre-dried by 4 Å molecular sieves and distilled from sodium benzophenone ketyl immediately before use. *N*,*N*′-Dicyclohexylcarbodiimide (DCC) and 4-dimethylaminopyridine (DMAP) were purchased from Chemical Reagent Co., Ltd, Jiangsu, China. Other chemicals were used as received from Sinopharm Group Chemical Reagent Co., Ltd, Shanghai, China.

2.2 Synthesis of azobenzene LC monomer

The azobenzene LC monomer, 6-(4-methoxy-4′-oxy-azobenzene)hexyl methacrylate (Azo-M), was synthesized according to the previous study [36]. The FTIR spectra of 4-hydroxy-4′-methoxyazobenzene (HMA), 1-bromo-6-(4-methoxy-azophenyl-4′oxy) hexane (BMAH), and Azo-M are shown in Figure S1. The ^{1}H NMR spectra of Azo-M and LCP are shown in Figures S2 and S5, respectively. The XRD result of LCP with Azo-M is shown in Figure S8.

2.3 Synthesis of POSS and AC-POSS macromonomer

POSS was synthesized according to previous studies [37,38]. The synthesis of AC-POSS macromonomer with THF as a solvent, 100 mg of amino POSS, 10 mL of acrylic acid, 0.3 g DCC, and 0.1 g DMAP were weighed. The reaction mixture was stirred under the protection of nitrogen with magnetic stirring at room temperature for 24 h. After the reaction, the white solid was precipitated by distilled water, washed with a large amount of distilled water to remove the excess acrylic acid, and then washed with acetone to remove a small amount of catalyst (DCC) resulting in functionalized POSS (AC-POSS). The FTIR spectra of POSS and the acrylic acid–modified polyhedral oligomeric silsesquioxane (AC-POSS) are shown in Figure S3. The XRD result of POSS is shown in Figure S7.

2.4 Synthesis of LCP/POSS (LCP-POSS) copolymer

Figure 1 shows the synthesis of LCP/POSS copolymer. LCP-POSSs with different contents were synthesized by adjusting the amount of substance POSS to 6-(4-methoxy-4′-oxy-azobenzene) hexyl methacrylate (Azo-M), which are presented in Tables 1 and 2. For example, for the synthesis of LCP–POSS-1 = 1:16, POSS (0.2 mmol) was dissolved in dried THF (5 mL), followed by the addition of Azo-M (3.2 mmol) and AIBN (0.136 mmol) under the protection of nitrogen. The reaction mixture was stirred at 65°C for 24 h. The mixture was precipitated with methanol. The final product was dried in a vacuum oven to obtain yellow solid. AC-POSS dissolved in water can be easily removed. A pure LCP-POSS was obtained by precipitation with methanol to remove excess azobenzene monomer and vacuum drying. Table 1 presents LCP-POSS copolymers with different synthesis ratios. The FTIR spectra of Azo-M, AC-POSS, LCP-POSS, and LCP are shown in Figure S4. Figure S6 shows the ^{1}H NMR spectrum of LCP-POSS.

3 Results and discussion

3.1 LC behavior of LCP-POSS polymer

LC birefringence behavior is a phenomenon in which a beam of light is incident into an anisotropic crystal, which is decomposed into two beams and refracted in different directions. Figure 2 shows the polarized optical micrographs of LCP and LCP-POSS. Figure 2(a) and (b) shows the LCP at 90°C and 30°C, respectively. Figure 2(c–f) shows LCP-POSS-1, 2, 3, and POSS at 30°C, respectively. Per previous study [38], the birefringence phenomenon of LCP can be observed in the process of heating and cooling, and LCPs exhibit the schlieren texture (Figure 2(b)) at the lower temperature. LCPs show bidirectional LC behavior. With increasing POSS content, the LC micro-area was reduced and the intersection point became vague. The LC micro zone became smaller (Figure 2(c) and (d)). When the molar ratio of LCP:POSS was 1:1, the birefringence was observed only in the cooling process, showing the one-way LC behavior (Figure 2(e)). The crystallization behavior of LCP-POSS could change through the addition of different contents of POSS.

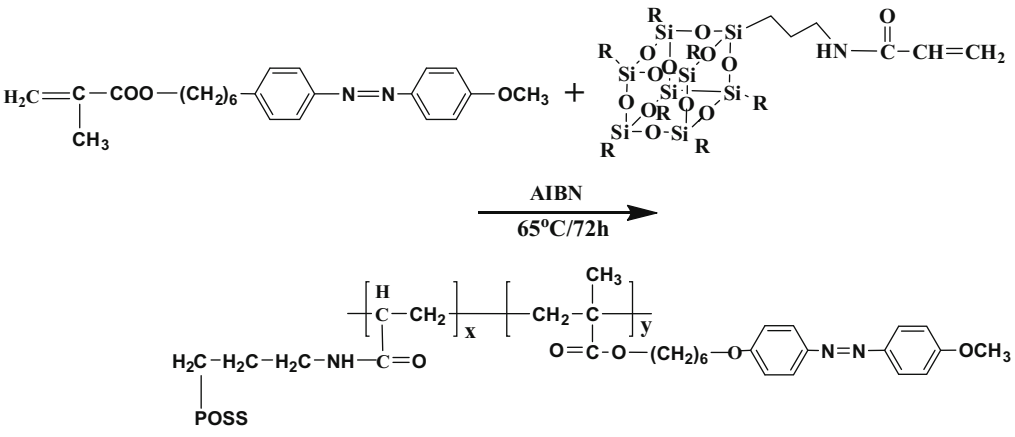

Figure 1: Synthesis of LCP-POSS.

Table 1: Synthesis of LCP-POSS with different proportions

Sample number	The ratio of the amount of substance POSS:LC	POSS-M	AzoM	AIBN
LCP	—	0	3.4 mmol	0.136 mmol
LCP-POSS-1	1:16	0.2 mmol	3.2 mmol	0.136 mmol
LCP-POSS-2	1:5	0.6 mmol	3.0 mmol	0.144 mmol
LCP-POSS-3	1:1	1.5 mmol	1.5 mmol	0.120 mmol
POSS	—	3.0 mmol	0	0.120 mmol

Table 2: Reaction condition and partial results of the synthesis of LCP-POSS liquid crystalline behavior

Sample number	Mn	Mw	PD
LCP	15,409	32,013	2.0776
LCP-POSS-1	5,826	14,763	2.5340
LCP-POSS-2	6,507	11,353	1.7447
LCP-POSS-3	2,706	3,832	1.3796
POSS	2,471	3,409	1.4161

Figure 3 shows the heating and cooling DSC curves of LCP and LCP-POSS. The LCP exhibited smectic–nematic transition (TSN) at 69.3°C and nematic–isotropic transition (TNI) at 106.1°C during heating. For LCP-POSS-1, the incorporation of 6.25 mol% POSS units into LCP increased TSN and TNI to 77.0°C and 112.76°C, respectively. For LCP-POSS-2, the incorporation of 20.0 mol% POSS units into LCP increased TSN and TNI to 86.9°C and 127.0°C (increment of 17.6–20.9°C), respectively. With the addition of LCP, an LC behavior appeared in LCP-POSS hybrid polymer in Figure 3. On one hand, a small amount of POSS with a high thermal stability could improve the thermal stability of LCP. The LC phase transition behavior of LCP-POSS-1 and LCP-POSS-2 occurred in the heating and cooling processes. As shown in Figure 3(b), during the cooling process, the phase transition temperature of LCP-POSS-1 appears to be 110.5°C and 73.5°C, respectively; the phase transition temperature of LCP-POSS-2 LC appears to be 125.8°C and 83.5°C, respectively. With further increasing the POSS content, a larger steric hindrance in the LCP-POSS influences the formation of LC-ordered structure. As per the curve *d* shown in Figure 3(b), only a one-way LC behavior of the LCP-POSS could be found during the cooling process.

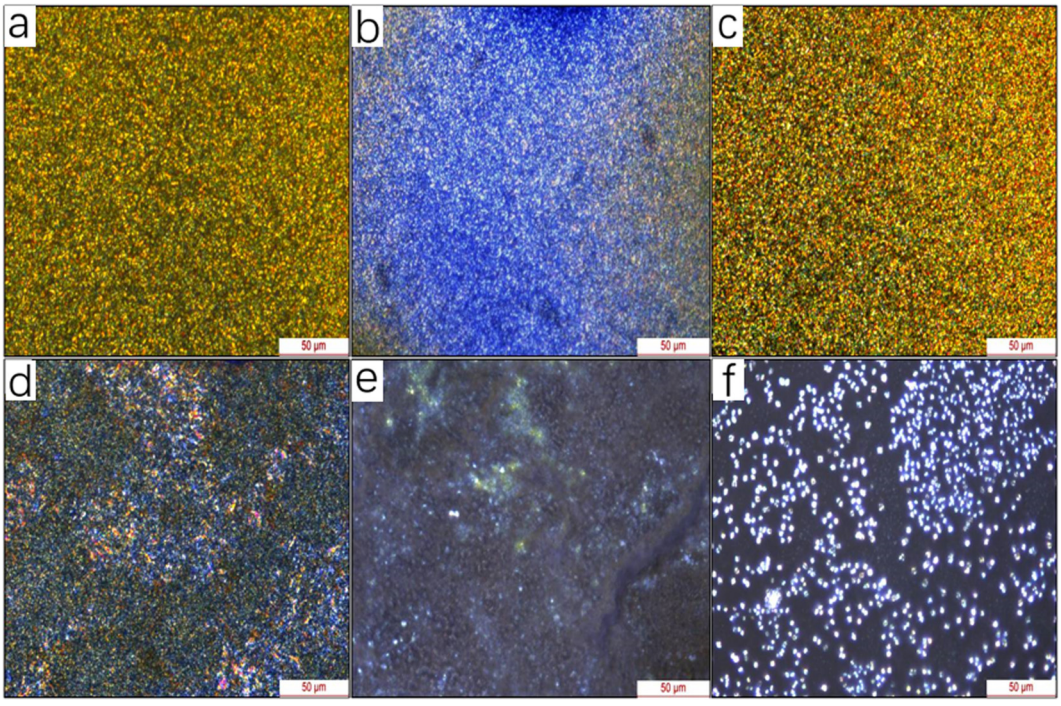

Figure 2: Polarized optical micrographs of LCP at 90°C (a), LCP at 30°C (b), POSS-LCP = 1 at 30°C (c), POSS-LCP-2 at 30°C (d), POSS-LCP-3 at 30°C (e), and POSS at 30°C (f).

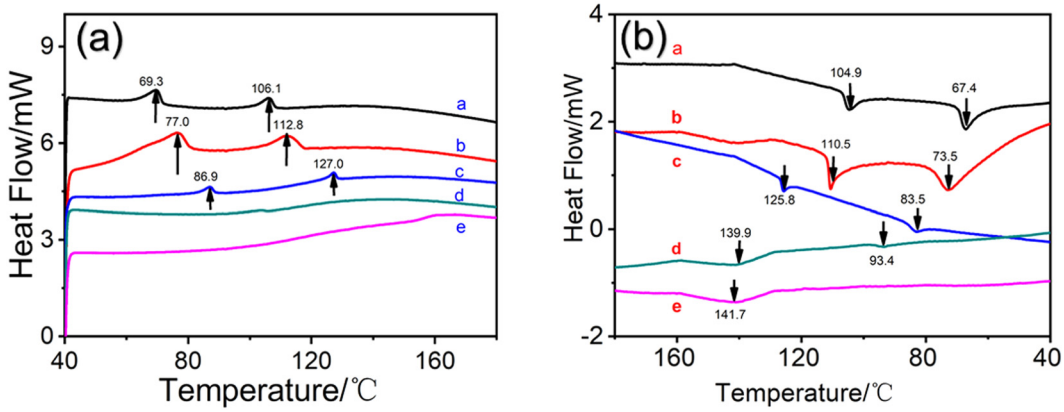

Figure 3: DSC heating and cooling curves of LCP (a), POSS:LCP = 1:16 (b), POSS:LCP = 1:5 (c), POSS:LCP = 1:1 (d), and POSS (e) at a rate of 20 K/min.

This phenomenon is consistent with the result of polarized optical microscope, where the crystallization texture could be observed only when cooling to 141.7°C.

3.2 Thermal stability

Figure 4 shows the thermal gravimetric (TG) curves of LCP, LCP-POSS-1, LCP-POSS-2, LCP-POSS-3, and POSS. In this study, the temperature at 10% decomposition is used as the initial decomposition temperature. The temperature at 10% decomposition shows the thermal stability of LCP and LCP-POSS, as presented in Table 3. Water can dissolve AC-POSS, which proves the synthesis of the LCP-POSS copolymer. The temperatures at 10% decomposition of LCP and POSS are 296.7°C and 343.4°C, respectively. The temperatures at 10% decomposition of LCP-POSS-1, LCP-POSS-2, and LCP-POSS-3 are 308.7°C, 317.4°C, and 327.8°C, respectively. It is clear that LCP has the lowest initial decomposition temperature, while POSS has the highest initial decomposition temperature. The result shows that the thermal decomposition temperature increases accordingly with the incorporation of the rigid cage-like POSS. Tanaka et al. [39] reported the use of unique organic–inorganic hybrid materials composed of octa-substituted polyhedral oligomeric silsesquioxane (POSS) cores as ionic liquid (IL) crystals. These materials could exist in the LC phase in a wide temperature range because of the stabilizing effect of the POSS core. The synthesized ion pairs composed of alkyl chain-substituted imidazolium and carboxylates of various lengths that were connected to the POSS core; then, the thermal properties of these materials were investigated. The highly symmetric structure of POSS contributes not only to the suppression of the molecular motion of the ion salts but also to the formation of regular structures, leading to thermally stable, thermotropic IL crystals [40]. The dispersion quality of nanoparticles has always limited the performance of polymer nanocomposites and coatings. Herein, the main purpose is to improve the dispersion quality of nanoparticles and overall properties in polyvinylidene fluoride (PVDF)/POSS nanocomposites fabricated through the spray-coating technique. POSS was added to PVDF/DMF solution at varying concentrations. The improved dispersion of POSS resulted in a significant enhancement in the crystallinity of PVDF from 29.8 to 59.5% according to the DSC results [41].

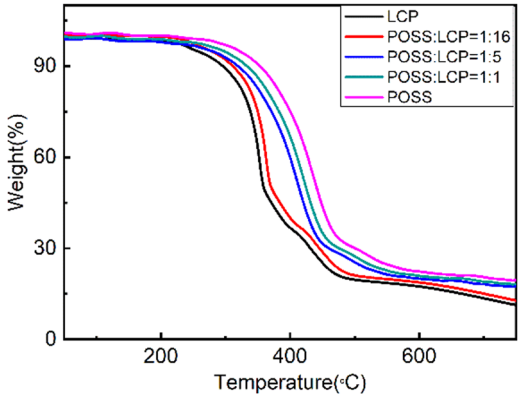

Figure 4: TG heating curves of LCP and LCP-POSS.

3.3 Photoresponsive properties

Different sample solutions were irradiated with 365 nm UV and visible light, and the variation of UV absorption spectrum with irradiation time was recorded. The

Table 3: Corresponding temperature of the LCP-POSS 10% decomposition

Sample number	The ratio of the amount of substance POSS:LC	LCP-POSS temperature 10% decomposition (°C)
LCP	—	296.7
LCP-POSS-1	1:16	308.7
LCP-POSS-2	1:5	317.4
LCP-POSS-3	1:1	327.8
POSS	—	343.4

photoisomerization behavior of azobenzene and the effect of LCP content on absorbance at the same concentration were studied. The corresponding results were obtained at different UV irradiation times. Figure 5 shows the UV-vis absorption spectra of LCP and LCP-POSS with different ratios (POSS:LCP = 1:16, 1:5, and 1:1) under the UV irradiation of 365 nm. The transition characteristic absorption peak of azobenzene at 358 nm belongs to the π–π* electron transition. With increasing UV irradiation time, the absorbance at 358 nm decreases rapidly, while the absorbance of the peaks at 450 and 310 nm increases slowly. The results indicate that azobenzene gradually changed from *trans*-configuration to *cis*-configuration until it reached the stable state. Figure 5 shows that the absorbance of azobenzene characteristic peaks decreases significantly with decreasing LCP content for LCP-POSS-1, LCP-POSS-2, and LCP-POSS-3 before UV irradiation. With increasing UV irradiation time, the absorbance of the corresponding absorption peak at 358 nm decreases rapidly, and the characteristic absorption peak of azobenzene is extremely low. The result suggests that *trans*-azobenzene transformed into *cis*-azobenzene. With the lower content of LCP, the absorbance of azobenzene characteristic peak decreases obviously after UV irradiation.

Figure 6 presents the UV-vis absorption spectra of the LCP and the LCP-POSS polymer solutions with different proportions (POSS-LCP-1, LCP-POSS-2, and

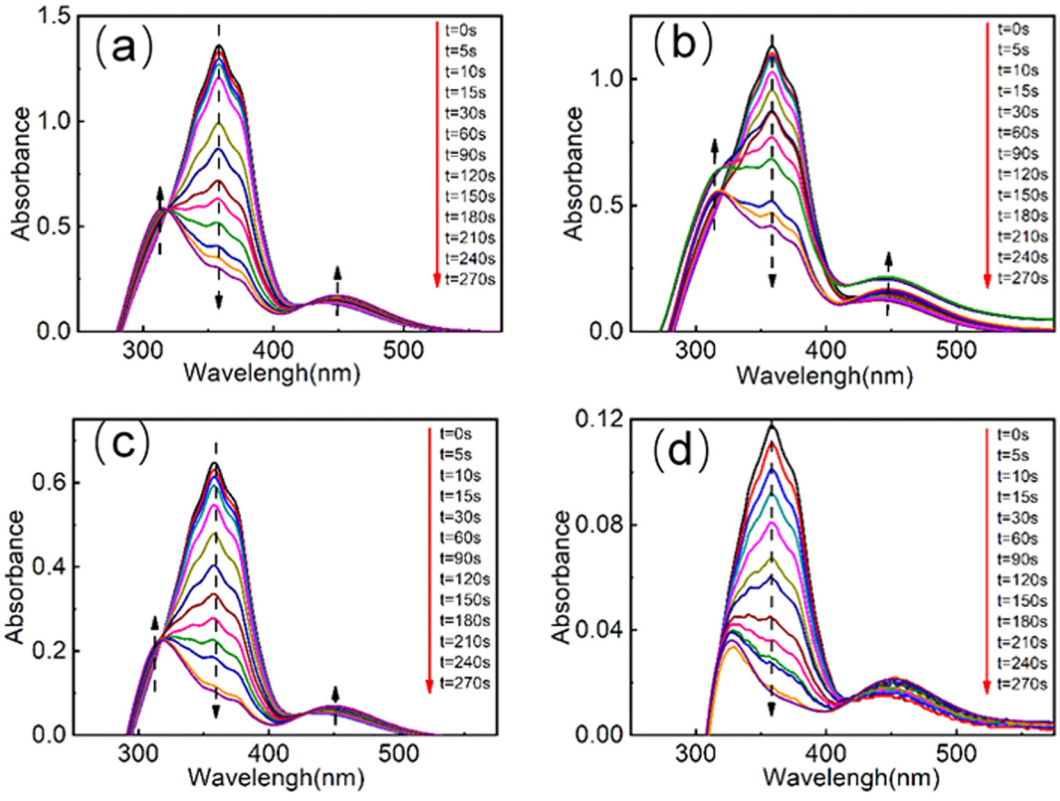

Figure 5: The UV-absorption of liquid crystalline polymer: (a) LCP, (b) LCP-POSS-1, (c) LCP-POSS-2, and (d) LCP-POSS-3 at different times with UV irradiation.

LCP-POSS-3) under visible light irradiation. The strong absorption peak at 358 nm corresponds to the π–π* electron transition of *trans*-azobenzene in LCP. The weak acromion at 450 nm belongs to the n–π* electron transition of *cis*-azobenzene. The weak absorption peak at 310 nm belongs to the n–π* electron transition of *cis*-isomer (short-axis parallel direction of *trans*-isomer). Under the visible light, the *cis* azobenzene transforms gradually, demonstrating that the isomerization of azobenzene is reversible.

The true POSS percentage in the copolymer could be calculated based on the maximum absorption values at 358 nm according to the Beer law, as presented in Table 4. The azobenzene content in different polymers is calculated: 83.03%, 47.61%, and 8.67% in LCP-POSS-1, LCP-POSS-2, and LCP-POSS-3, respectively.

The first-order reaction kinetics was used to study the influence of the *trans–cis* isomerization reaction with the different POSS contents as presented in Table 5. A_0 is the absorbance before the light ($t = 0$) at 358 nm, A_t is the absorbance at the time of the light t, A_∞ is the absorbance at the light $t = \infty$, and K is the first-order reaction rate constant of the *trans*-to-*cis* transformation (π–π* electron transition) [42].

Table 4: Percentage compositions of the actual polymerized liquid crystal

Sample number	The absorption peak of polymers at 358 nm	The azobenzene content in polymers (%)
LCP	1.361	100
LCP-POSS-1	1.130	83.03
LCP-POSS-2	0.648	47.61
LCP-POSS-3	0.118	8.67

Table 5: Result of dynamic behavior of *cis–trans* isomerism

Sample number	Linear equation	R^2
LCP	$y = 0.01129x - 0.05928$	0.98402
LCP-POSS-1	$y = 0.00876x - 0.06654$	0.98548
LCP-POSS-2	$y = 0.008x - 0.04439$	0.98628
LCP-POSS-3	$y = 0.0052x - 0.00307$	0.98647

$$\ln\left[(A_\infty - A_t) - (A_\infty - A_0)\right] = -kt$$

where A_∞ is the absorbance at 360 nm with the UV irradiation time until the balance state, A_t is the

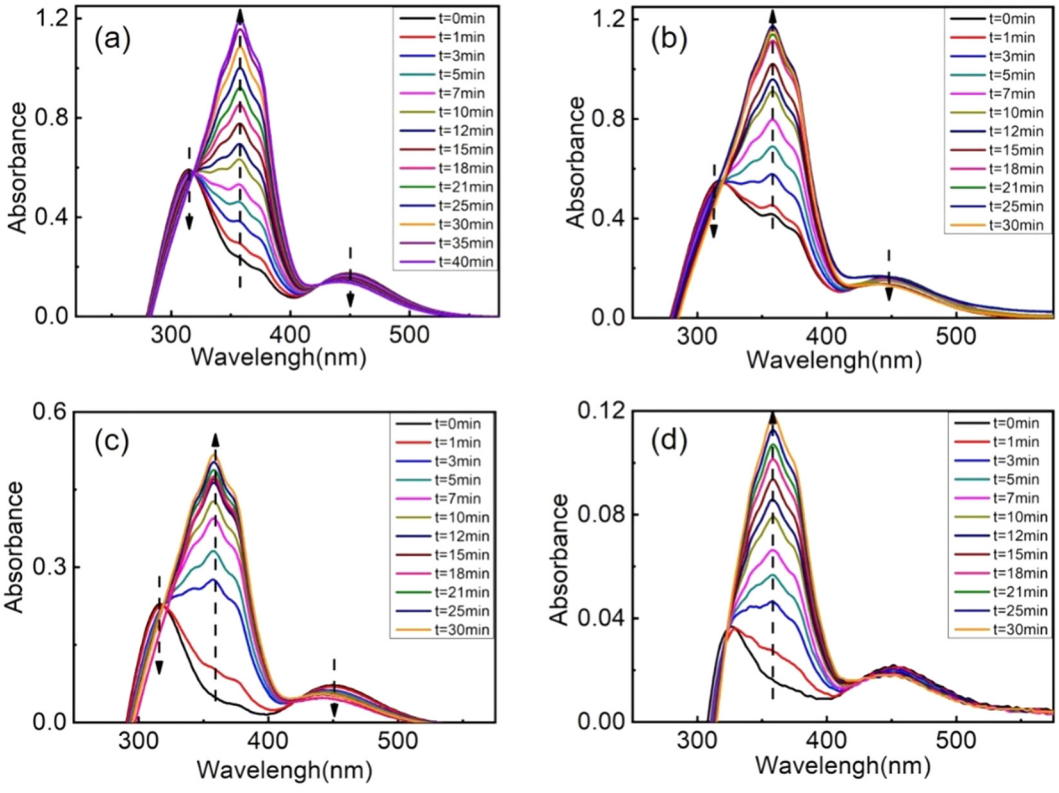

Figure 6: The UV absorption of liquid crystalline polymer: (a) LCP, (b) LCP-POSS-1, (c) LCP-POSS-2, and (d) LCP-POSS-3 at different times with visible light.

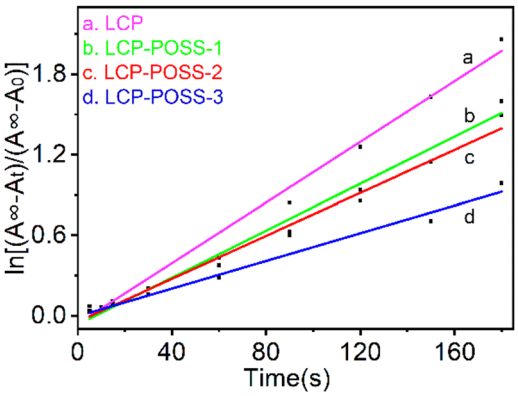

Figure 7: First-order kinetics curves of *cis–trans* isomerization.

absorbance at 360 nm with the UV irradiation time t, and A_0 is the absorbance at 360 nm without the UV irradiation. The aforementioned formula is the light reaction kinetics equation, as presented in Table 5. These approximately straight lines are obtained by the formula, and the slopes are the reaction rate constants (k) of polymer isomerization. Introducing POSS to LCP decreased the rate constant of *cis–trans* photoisomerization to some extent. It can be seen that the isomerization reaction rate constant decreases with the addition of POSS (Figure 7). The isomerization reaction rate constants of LCP, LCP-POSS-1, LCP-POSS-2, and LCP-POSS-3 are 0.0112×10^{-4}, 0.0052×10^{-4}, 0.008×10^{-4}, and 0.0086×10^{-4}, respectively. This result suggests that the addition of POSS to LCP structure, to some extent, weakened the isomerization reaction rate constant of LCP. Due to the structural ordering of POSS, the incorporation of POSS to LC has been extensively investigated. The LC element was incorporated into POSS to produce LCP-POSS hybrid, in which the degree of order increase, by Goodby and coworkers [43,44]. The LC phase was transformed from nematic phase to smectic phase with increasing LC temperature. Then, they incorporated chiral POSS molecules to LC, which increased the LC phase temperature [43,44]. The azobenzene LCP-POSS copolymers that have increased the LC temperature and reversible light-responsive properties were synthesized for the first time in our work. These hybrid copolymers with excellent LC behavior and light-responsive properties may be applicable in the LC display area. In our work, the incorporation of 47.61% azobenzene increased the structural ordering of LCP-POSS with the higher LC phase transition temperature, while the light-responsive property is basically unaffected.

4 Conclusions

The LCP-POSS with LC properties, light-responsive properties, and good thermal stability was synthesized through radical polymerization of modified AC-POSS and azobenzene LC, in which water-soluble AC-POSS is easy to remove after reaction. Due to the confinement of the rigid cage-like POSS, LCP-POSS exhibits better thermal stability and higher phase transition temperature. As the content of POSS gradually increases, the thermal stability of LCP-POSS gradually increased and the temperature at 10% decomposition of LCP-POSS-3 was 31.1°C higher than LCP. The LC phase transition temperature of LCP-POSS increased from 104.9°C to 139.9°C, and the polarized optical micrograph results further confirm the results. Incorporating about 53% POSS to LCP could not only keep the LC phase structure but also improve the thermal stability of LCP. As the content of azobenzene further decreased to 8.67%, the LC properties of the LCP-POOS-3 indicated the one-way LC phase behavior. Because of the steric hindrance effect, the addition of POSS to the LCP matrix reduces the *cis–trans* isomerization constant of azobenzene. However, the reversible photoresponsive behavior was still preserved, which has important application in nanodevice, optical switch, information storage, and liquid crystal display.

Acknowledgments: This work was supported by the Natural National Science Foundation of China (51303049) and Key projects of Hubei Provincial Department of Education (D20191404). The university started the doctoral program BSQD12116. Thanks to Hubei University of Technology for their help with the DSC, UV, and FTIR measurements.

Conflict of interest: The authors declare no conflict of interest regarding the publication of this paper.

References

[1] David BC, Paul DL, Franck R. Recent development in the chemistry of cubic polyhedral oligo silsesquioxanes. Chem Rev. 2010;110(4):2081–173.
[2] Karimi A, Vatanpour V, Khataee A, Safarpour M. Contra-diffusion synthesis of ZIF-8 layer on polyvinylidene fluoride ultrafiltration membranes for improved water purification. J Ind Eng Chem. 2019;73(2):95–105.
[3] Mishra K, Singh RP. Quantitative evaluation of the effect of dispersion techniques on the mechanical properties of

polyhedral oligomeric silsesquioxane (POSS)–epoxy nanocomposites. Polym Composite. 2018;39(1–2):2445–53.
[4] Sagar Roy, Roumiana S. Functionalized carbon nanotube interfacial interaction nanocomposites physical properties thermal properties. Nanotechnol Rev. 2018;7(2):475–85.
[5] Tong X, Wang G, Soldera A. How can azobenzene block copolymer vesicles be dissociated and reformed by light. J Phys Chem B. 2005;109(3):20281–7.
[6] Wu Y, Tang B, Liu K. Enhanced flexural properties of aramid fiber/epoxy composites by graphene oxide. Nanotechnol Rev. 2019;8(1):484–92.
[7] Lubomir L, Barbora L, Martin V. Materials characterization of advanced fillers for composites engineering applications. Nanotechnol Rev. 2019;8(2):503–12.
[8] Ni Y, Zheng SX, Fisher MA. Novel Photocrosslinkable polyhedral oligomeric silsesquioxane and its nanocomposites with poly(vinyl cinnamate). Chem Mater. 2004;16(1):5141–8.
[9] Zheng L, Hong S, Cardoen GE. Polymer nanocomposites through controlled self-assembly of cubic silsesquioxane scaffolds. Macromolecules. 2004;37(3):8606–11.
[10] Lee A, Sugahara B, Chuzo B. New approach in the synthesis of hybrid polymers grafted with polyhedral oligomeric silsesquioxane and their physical and viscoelastic properties. Macromolecules. 2005;38(4):438–44.
[11] Strachota A, Kroutilova IR, Jana KR. Epoxy networks reinforced with polyhedral oligomeric silsesquioxanes (POSS) thermomechanical properties. Macromolecules. 2004;37(5):9457–64.
[12] Kim KM, Yu KO, Chujo YS. Synthesis of organic–inorganic star-shaped polyoxazolines using octafunctional silsesquioxane as an initiator. Polym Bull. 2003;49(2):341–8.
[13] Senthil KMS, Mohana SRN, Sampath PS. Effects of nano materials on polymer composites – an expatiate view. Rev Adv Mater Sci. 2014;38(1):40–54.
[14] Guo SH, Fu DW, Jin Z. Applications of polymer-based nanoparticles in vaccine field. Nanotechnol Rev. 2019;8(3):143–55.
[15] Pielichowski K, Njuguna J, Janowski B, Pielichowski J. Fluorinated polyhedral oligomeric silsesquioxanes (F-POSS). Adv Polym Tech. 2006;201(2):225–63.
[16] Laine RMJ. Preparation and characterization of transparent polyimide/silica composite films by a sol–gel reaction. Chem Mater. 2005;15(2):3725–806.
[17] Stanley EA, Erin SB, Connle M. Structure of hybrid polyhedral oligomeric silsesquioxane propyl methacrylate oligomers using lon mobility mass spectrometry and molecular mechanics. Chem Mater. 2005;17(1):2537–45.
[18] Krishnan PSG, He C. Octa(maleimido-phenyl) silsesquioxane copolymers. J Polym Sci Pol Chem. 2005;43(3):2483–94.
[19] Kenji W, Take-aki M. Preparation of novel materials for catalysts utilizing metal-containing silsesquioxanes. Catal Surv Asia. 2005;4(1-2):229–41.
[20] Kannan RY, Salacinski HJ, Butler PE. Polyhedral oligomeric silsesquioxane nanocomposites: the next generation material for biomedical applications. Acc Chem Res. 2005;38(4):879–84.
[21] Kang JM, Cho HJ, Lee JI. Highly bright and efficient electroluminescene of new PPV derivatives containing polyhedral oligomeric silsesquioxanes (POSSs) and their blends. Macromolecules. 2006;39(3):4999–5008.
[22] Tanaka K, Adachi S, Chujo Y. Side-chain effect of octa-substituted POSS fillers on refraction in polymer composites. J Polym Sci Pol Chem. 2010;48(3):5712–7.
[23] Kim KM, Yu KO, Chujo YS. Polymer hybrids of functionalized silsesquioxanes and organic polymers utilizing the sol–gel reaction of tetramethoxysilane. J Polym Sci Pol Chem. 2002;39(2):4035–43.
[24] Fan XH, Zhu YF, Zhang ZY, Shen ZH. Synthesis and phase behavior of a POSS-containing jacketed polymer. CAJ. 2014;29(2):359–40.
[25] Zhang C, Laine RM. Synthesis of organic-inorganic star-shaped polyoxazolines using octafunctional silsesquioxane as an initiator. Chem Mater. 2003;13(2):3653–62.
[26] Islam MR, Bach LG. Synthesis and characterization of poly (HEMA-co-MMA)-g-POSS nanocomposites by combination of reversible addition fragmentation chain transfer polymerization and click chemistry. J Appl Polym Sci. 2013;127(5):1569–77.
[27] Feng Z, Lin L, Yan Z. Dual responsive block copolymer micelles functionalized by NIPAM and azobenzene. Macro Rap Comm. 2010;31(4):640–4.
[28] Wang YP, Han P, Xu HP. Photocontrolled self-assembly and disassembly of block ionomer complex vesicles: a facile approach toward supramolecular polymer nanocontainers. Langmuir. 2010;26(1–2):709–15.
[29] Wang XT, Liu C, Li ZH. Thermal and photo dual-responsive core–shell polymeric nanocarriers with encapsulation of upconversion nanoparticles for controlled anticancer drug release. J Phys Chem C. 2019;123(16):10658–65.
[30] Tanaka T, Ogino H, Iwamoto M. Photochange in pore diameters of azobenzene-planted mesoporous silica materials. Langmuir. 2007;23(6):11417–20.
[31] Wang XT, Liu XP, Wang L. Synthesis of yolk-shell polymeric nanocapsules encapsulated with monodispersed pconversion nanoparticle for dual-responsive controlled drug release. Macromolecules. 2018;51(2):10074–82.
[32] Fujiwara M, Akiyama M, Nomura R. Photoinduced acceleration of the effluent rate of developing solvents in azobenzene-tethered silica gel. ACS Nano. 2008;2(1):1671–81.
[33] Chen L, He CL, Huang YG. POSS-based fluorinated azobenzene-containing polymers: photo-responsive behavior and evaluation of water repellency. J Appl Polym Sci. 2016;20(2):1–9.
[34] Miniewicz A, Tomkowicz M, Karpinski P, Sznitko L. Light sensitive polymer obtained by dispersion of azo-functionalized POSS nanoparticles. Chem Phys. 2015;1(3):1–25.
[35] Zhao Z, Wang X, Qiu J. Three-dimensional graphene-based hydrogel/aerogel materials. Rev Adv Mater Sci. 2014;36(2):137–51.
[36] Haitjema HJ, Buruma R, Alberd GOR, Tan YY, Challa G. New photoresponsive (meth)acrylate (co)polymers containing azo-benzene pendant side groups with carboxylic and dimethylamino substituents-II. Synthesis and characterization of polymers and copolymers. Eur Polym. 1996;32(1):1447–551.
[37] Yoshino TK, Kondo MZ, Mamiya JI. Three-dimensional photomobility of crosslinked azobenzene liquid-crystalline polymer fibers. Adv Mater. 2010;22(3):1361–3.

[38] Guo HQ, Meador MAB, McCorkle L. Polyimide aerogels cross-linked through amine functionalized polyoligomeric silsesquioxane. ACS Appl Mater Interfaces. 2011;3(2):546–52.
[39] Tanaka K, Ishiguro F, Jeon J. POSS ionic liquid crystals. NPG Asia Mater. 2015;7(3):174–9.
[40] Feher FJ, Budzichowski TA, Blanski RL, Weller KJ. Facile syntheses of new incompletely condensed polyhedral oligosilsesquioxanes: $[(c\text{-}C_5H_9)_7Si_7O_9(OH)_3]$,$[(c\text{-}C_7H_{13})_7Si_7O_9(OH)_3]$, and $[(c\text{-}C_7H_{13})_6Si_6O_7(OH)_4]$. Organometallics. 1991;10(2):2526–8.
[41] Mehrdad K, Ardeshir S, Hossein A. Improving nanoparticle dispersion and polymer crystallinity in polyvinylidene fluoride/POSS coatings using tetrahydrofuran as co-solvent. Prog Org Coat. 2019;140(1):65–78.
[42] Yang YK, Xie XL, Wu JG. Multiwalled carbon nanotubes functionalized by hyperbranched poly(urea-urethane)s by a one-pot polycondensation. Macromol Rapid Comm. 2006;27(4):1695–701.
[43] Zhong TJ, Mandle RJ, Goodby JW, Zhang LY, Zhang CH. Comparative studies of polymer-dispersed liquid crystal films *via* a thiol-ene click reaction. Adv Polym Tech. 2019;30(2):2781–9.
[44] Tong X, Wang G, Soldera A. How can azobenzene block copolymer vesicles be dissociated and reformed by light. J Phys Chem B. 2005;109(3):20281–7.